Journal of Photopolymer Science and Technology
Volume 28, Number 6 (2015) 747 – 754© 2015SPST

Development of a High-Intensity UV Exposure Apparatus under a High-Pressure CO_2 Gas Atmosphere to Manufacture Large-Area Porous Ultralow-k Polyimide Substrates for Flexible Print Circuits

Kentaro Taki[1]*, Hiroshi Ito[2]

[1]Chemical and Materials Engineering Course, School of Natural Systems, College of Science and Engineering, Kanazawa University, Kakumacho, Kanazawa, Ishikawa, 920-1192, Japan
[2]Department of Polymer Science and Engineering, Yamagata University, 4-3-16, Jonan, Yonezawa, Yamagata, 992-8510, Japan.

Ultralow-k (dielectric constant) films are promising substrates for next-generation flexible print circuits. Introducing numerous pores into the film can effectively reduce the substrate's dielectric constant because the relative dielectric constant of air is smaller than that of any polymer substrate. We recently developed a short-cycle time process employing high-pressure CO_2 and the CO_2-tertiaryamine zwitterions in polyimide precursor solutions to create 1-3 μm pores of >70% porosity. However, the film size was limited to 30 × 30 mm^2. A larger film (70 × 150 mm^2) was required to measure the signal attenuation of an electrical circuit on a porous PI film as a next-generation flexible cable. In this paper, the developed process was scaled up to obtain 10-fold-larger ultralow-k films of porous polyimide. The process involved a high-intensity UV lamp, thick-quartz window and hydraulically movable sealing plate and produces 70 × 150 mm^2 films, which was a suitable size for high-speed data communication transmission tests. The preliminary results of building up a printed circuit on the porous substrate and signal attenuation measurements at 20 GHz demonstrated that the low-k porous PI substrate reduced the signal attenuation compared to a non-porous substrate with the same cross-sectional line area.

Keywords: polyimides, photopolymerization, macroporous polymers, dielectric properties, films

1. Introduction

In the electronics industry, polyimide (PI) films are utilized in the production of flexible printed cable (FPC) in electronic devices because of the inherently high heat resistance, flexibility and chemical stability of PI [1]. With the increasing transmission speed of mobile information devices, e.g., cellular and smart phones, PI FPCs require a lower relative dielectric constant to decrease the signal attenuation [2-5]. There are two strategies for reducing the dielectric constant of PI. One strategy involving chemical modifications of the PI backbone and side chains has been examined in recent review articles [5,6]. The incorporation of fluorinated substituents into polymers decreases their dielectric constant because of the low dipole moment and the low polarizability of the C–F bond. The dielectric constant of the fluorinated PI is limited to 2.7-3.0, and the poor adhesion between the copper substrate and the fluorinated polymer remains a significant challenge.

An alternative strategy involves the introduction of voids into PI films [5]. Pioneering studies on the introduction of 10 nm-sized pores into PI were conducted by Hedrick [7], who designed a block copolymer system that could be pyrolyzed at high temperatures to form voids in a PI matrix for applications such as insulators in integrated circuits. Voids were successfully formed in the PI, although the porosity was limited by the small number of pores. Another approach to forming pores involves the physical foaming technique, wherein CO_2 gas

Received September 28, 2015
Accepted October 23, 2015

dissolved in a polymer matrix is thermally phase-separated to induce bubble nucleation in the glassy and rubbery state of the polymer [8,9]. The dielectric constant achieved using this method is 1.77, which is known as the ultralow-k level [9]. A supercritical fluid-assisted extraction technique has been applied to remove mesoscale domains in a PI matrix, whereas the remaining domains are allowed to become voids [10]. The concept was further studied for poly(methyl methacrylate) and polystyrene [11]. Although the process used to create mesosized pores is highly sophisticated, the complete extraction of all domains is considered to be impossible. The resulting incomplete extraction may be unfavorable for the application of such materials in electronic devices.

Water-borne porous PI has been prepared via the condensation of water vapor onto the PI solution spun on a substrate [4]. The micron-sized water droplets on the substrate correspond to the porogen. This method resulted in a decrease in the dielectric constant of porous films to 1.7, although a 48 h process was required for water droplets to form in the porous films.

The formation of meso-sized pores in a PI matrix by the addition of polyhedral oligomeric silsesquioxane (POSS) as an organic-inorganic hybrid porogen has been reported by several authors [12-15]. Inorganic porogens, such as hollow silica particles and mesoporous silica, were effectively used to reduce the dielectric constant [16-21]. Leaching out of lithium chloride is another method of preparing pores [22]. Compounding the porogens produces films with relatively low porosity; however, it is difficult to achieve a porosity greater than 70% because of the presence of porogen shells.

To decrease the dielectric constant by increasing the porosity further while achieving a short processing time, this study builds upon our recently reported approach in which UV curable monomers and a CO_2 solution were phase-separated to form a transient porous structure that was then solidified by rapid photopolymerization [23]. Moreover, the photopolymerization followed by unidirectional freezing enabled the creation of honeycomb porous structures from the UV-curable monomer/solvent /photoinitiator solid-liquid phase separation [24]. This approach is useful for creating macroporous materials for systems that could be phase-separated and photopolymerized. The main advantage of this approach is the reduction in processing time and increase in porosity. The photopolymerization can create a stable porous structure instantaneously, whereas the conventional process that utilized diffusion requires significantly more time to achieve a stable porous structure.

Recently, we discovered a new system suitable for generating an ultralow-k PI film of high porosity using a short processing step [25]. Figure 1 shows the porous PI film formation process from the poly(amic acid) (PAA) solution, CO_2 and the UV-curable *tert*-amine monomer.

A mixture of PI precursor, solvent and UV curable monomer/photoinitiator was used as a negative tone PI resist. The monomer and solvent were dispersed in the PAA solution after a certain amount of solvent vaporized.

When the high-pressure CO_2 was introduced, the monomer and CO_2 formed zwitterion salts. Upon exposure to CO_2, phase separation was immediately observed, resulting in the formation of solvent droplets in the mixture. The solvent droplets were formed in domains surrounded by the salt species. The UV irradiation then induced the polymerization of the monomers under high-pressure CO_2. The transient structure of the phase-separated mixture consisting of droplets in a wet film was solidified by the photopolymerization of the UV-curable monomer using UV irradiation. After the CO_2 pressure was decreased, the solvent droplets vaporized to form pores in the film.

The pore formation and solidification process was completed within 2 min. The porous PI precursor obtained was transformed into porous PI via a heat treatment. Although two hours of

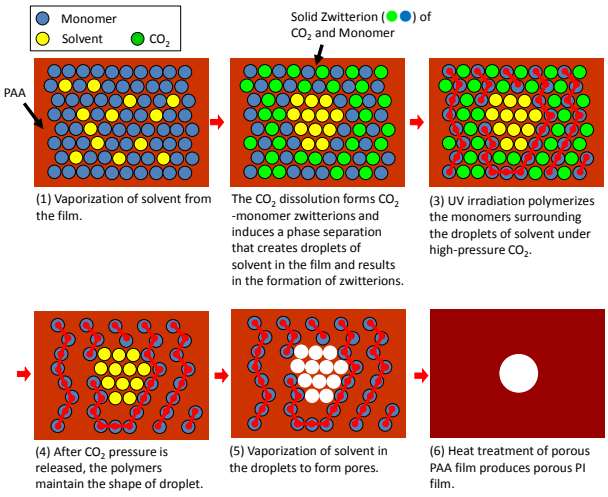

Fig. 1. Formation of porous PI films from a PAA solution, CO_2 and a UV-curable *tert*-amine monomer. Reproduced with permission [25].

thermal imidization was required, the developed process was considerably faster than in a previous study [4]. The relative dielectric constant and loss tangent of the porous PI films were measured at 20 GHz. The relative dielectric constant decreased dramatically up to 1.4 with a porosity of 80%. However, the size of film available to produce was limited to 30 × 30 mm^2. A larger size e.g., 70 × 150 mm^2 film was required to draw an electrical circuit using a typical production process and measure the signal attenuation of an electrical circuit on the porous PI film.

In this study, the developed process was scaled-up to obtain a 10-fold larger ultralow-k film of porous polyimide. The apparatus consists of a high-intensity UV lamp, thick-quartz window and hydraulic piston and produced 70 × 150 mm^2 size films, which was a suitable size for transmission tests of high-speed data communication.

2. Experimental

2.1. Materials

The PI precursor (PAA) was synthesized using a dry three-neck flask [25]. Approximately 0.505 g (2.52 mmol) of 4,4'-diaminodiphenyl ether was dissolved in 5.5 g of *N*,*N*-diethylacetamide in the three-neck flask using a mechanical agitator under an atmosphere of nitrogen gas. Subsequently, 0.550 g (2.52 mmol) of pyromellitic dianhydride was added to the flask. The polymerization was allowed to proceed for 8 h, producing a yellow-colored viscous liquid. Approximately 1.58 g (8.53 mmol) of UV curable monomer, 2-(diethylamino)ethyl methacrylate, and 0.201 g (0.577 mmol) of photoinitiator, diphenyl(2,4,6-trimethylbenzoyl)phosphine oxide, were added to 6.56 g of the precursor solution and stirred until a homogeneous solution was obtained. The solution was cast on a copper substrate (300×210 mm^2) using a wired-bar and a pre-heated (40 ^oC) automated coater (Imoto Machinery, Kyoto, Japan). The wet film was approximately 100 μm thick.

2.2. Apparatus

In our previous study, the apparatus consisted of two t25×ϕ65 mm cylindrical quartz windows to realize through-view observation and UV exposure simultaneously. The cast film was placed between the windows by opening the window holder and upper window [25]. However, the large-area production system requires t95×ϕ220 mm quartz glass to hold 6.5 MPa of CO_2 pressure and realize a ϕ165 mm chamber area. The total weight of the window holder and window was 310 kg, which was not suitable to remove every experiment. Therefore, the developed process consisted of a window and hydraulic-piston metal plate. Figure 2 shows a schematic and picture of the developed process. The high-pressure chamber could hold the high-pressure CO_2 with the fixed window and movable plate.

(a)

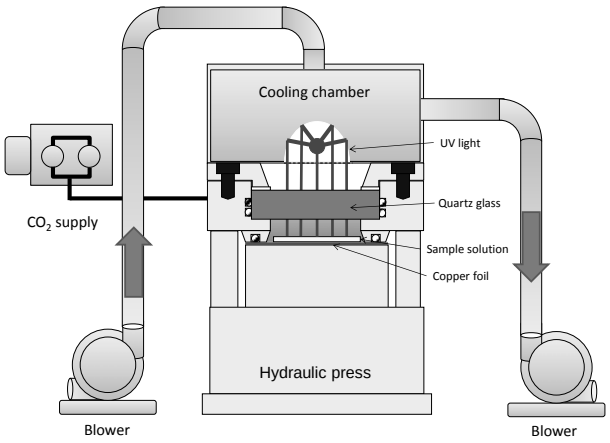

(b)

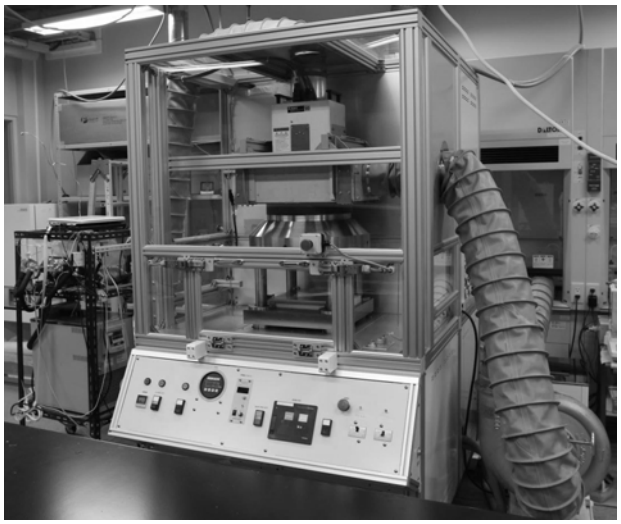

Fig. 2. (a) Schematic diagram, (b) picture of the developed apparatus for the large-area porous PI process. The apparatus was built by a joint project with Fusion-UV Japan (Tokyo, Japan), Tamaseiki Kogyo (Tokyo, Japan) and Imoto Machinery (Kyoto, Japan).

When the sample was placed in the chamber, the movable plate was moved down to open the chamber by releasing the hydraulic pressure. Then, the movable plate was returned up to seal the

chamber. The contact area between the plate and window holder was sealed by a silicone O-ring. The sidewall of the window was held and put into contact with the window holder with two other silicone O-rings. The silicone O-ring was transparent, resistant to UV light and able to easily release CO_2. The temperature of the chamber must be higher than 40°C to vaporize the high-pressure CO_2. The chamber was heated by a hot-air circulator. If the high-pressure CO_2 was liquefied in the chamber, the O-rings were significantly damaged. The circumference of top of the window was held by a PTFE gasket wrapped with aluminum foil, which was critical to protect the gasket against UV light.

Because the distance between the UV light and cast film was longer than 250 mm, the strongest commercially available UV lamp (Light Hummer 10, 240 W/cm, Fusion UV, Japan) was installed. UV intensity on the cast film 250 mm from UV lamp could be achieved at 200 mW/cm^2.

A programmable logic controller (PLC, Keyence, Japan) was installed to operate the time sequence of the developed apparatus. The sequence progressed as follows:

(1) The cast film was manually placed on the pre-heated (40 °C) movable plate.

The pre-drying was performed if required for the desired time.

(2) The movable plate was lifted up to the pre-heated (40 °C) window holder by the hydraulic press. (1 min)

(3) CO_2 gas was loaded into the chamber by opening an automated valve. The CO_2 pump was started to increase the CO_2 pressure up to 6.5 MPa. When the CO_2 gas was introduced, the CO_2-*tert*-amine monomer zwitterion formed, and the phase separation occurred immediately. (1 min)

(4) The UV lamp was ignited to irradiate UV light onto the cast film. UV irradiation induced the photopolymerization of the *tert*-amine monomer in the cast film and froze the transient structure of the phase separation. (1 min)

(5) CO_2 pressure was released by opening another automated valve to atmospheric pressure. (3 min)

(6) The movable plate was dropped down gently to open the chamber. The porous PAA film was taken out from the chamber.

2.3. Imidization of the Porous PAA Film

The transformation from the precursor to a porous PI film was achieved using a heat treatment in a nitrogen-flushed oven (DN610I, Yamato Scientific, Tokyo, Japan) using the following temperature gradients: (1) 40 °C for 120 min, (2) 3 °C/min to 110 °C for 60 min, and (3) 3 °C/min to 320 °C for 60 min under 20 L/min of nitrogen.

2.4. Development of the Electrical Circuit

The porous film was exposed to UV irradiation to improve the hydrophobicity of the surface. The film was coated with a precursor of electroless plating. The precursor was activated by heat treatment. Electroless plating and subsequent electroplating of copper were performed on the surface of the porous polyimide in the plating solution. The porous film was completely dried.

The dry-film resist was applied to the copper substrate (not the electroplated side) of the porous polyimide. The pattern of the electrical circuit was exposed, and the circuit was developed. The electrical circuit was developed at a company (Multi, Japan). A cross-section polisher was used to expose the cross-section of both the circuit and polymers. The surface and cross-section were observed using a field emission scanning electron microscope.

2.5. Measurement of the Signal Attenuation

The signal attenuation of a high-frequency signal was measured using micro contact probes. The micro contact probes were attached to either end of the circuit on the substrate. The signal range was from 10 MHz to 20 GHz. A network analyzer (Agilent 8361A) was used. The temperature was 26 °C, and the relative humidity was 50%.

3. Results and Discussion

The goal of the developed process was to build an enlarged area of porous polyimide films. It was realized by introducing a large and thick quartz window. Furthermore, this larger-scale process enabled the prepared porous films to be more conformal and uniform. The process was operated by the sequencer automatically, and the manual operation did not intervene in the process.

Figure 3 shows an optical picture of the porous PI film produced by the developed process. The size of the porous PI film was 150 × 70 mm^2, which is sufficient to build up the electrical circuit. The film was approximately 40 μm thick. The film has a glossy surface, which indicates that the surface is a conformal skin layer. Uneven coloring of the surface was caused by the unevenness of the drying. The film was dried three times through pre-drying after casting, drying in the chamber and

drying in the imidization process. The solvent (DMAc) and residual monomer were bled out from the film in the imidization process. The monomers were thermally polymerized and degraded and remained on the surface with the increase in temperature up to 320 ^{o}C. The residual stress caused by the shrinkage was relatively small compared with the non-porous PI film. The non-porous film was curled after the heat treatment of imidization. The porous film was not curled because the residual stress was reduced by pore volume.

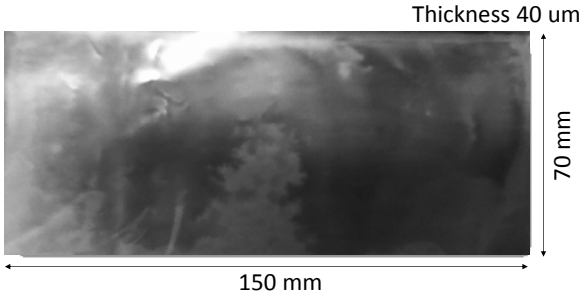

Fig. 3. Optical picture of the porous PI film produced by the developed process.

Figure 4 shows the SEM micrographs of the cross-section of a porous PI film prepared at 6.5 MPa of CO_2 pressure and UV Level 80 (~130 mW/cm^2). Most of the pores are isolated from each other, but some pores were interconnected. The shapes of the pores were ellipsoidal, with the long axis along the horizontal direction and the short axis along the vertical direction.

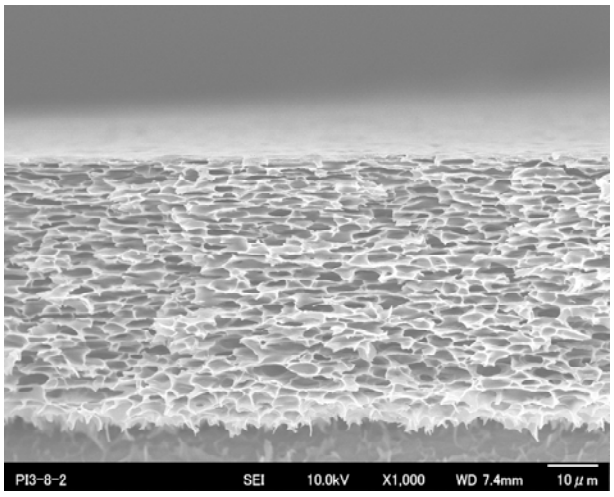

Fig. 4. SEM micrograph of the cross-section of a porous polyimide film prepared at 6.5 MPa of CO_2 pressure and UV Level 80.

When the pores were formed in the PAA cast film, the shape of the pores had been symmetrical [25]. When the pores were formed in the PAA cast film, the shape of the pores had been symmetrical [25]. Then, the film was transformed to polyimide in the oven. The shrinkage along the normal direction to the film was more prominent during the imidization reaction because the film surface was free. The pore eventually became ellipsoidal.

Figures 5(a)-(d) show the effect of pre-drying time on the porous structure of the PI film. The pre-drying time was the time for evaporating the solvent on the pre-heated movable plate in the sequence (1) of the 2.2 Apparatus section.

The thin copper film under the porous PI film was peeled off by bending the film under a liquid nitrogen bath. The upper side was exposed to the UV and CO_2. The bottom side had been cast with the porous PI film.

The film thickness and pore diameter are listed in Table 1. The thicknesses of the porous films were 44 μm for 0 min, 41 μm for 3 min, 18 μm for 5 min and 12 μm for 7 min. The average pore diameters were 2.5 ± 0.5 μm for 0 min, 2.1 ± 0.2 μm for 3 min, 1.7 ± 0.2 μm for 5 min. The average pore diameter was 0.8 ± 0.1 μm while the number of pores was scarce for 7 min.

Both the film thickness and average pore diameter were reduced by increasing the pre-drying time. As shown in Figure 1, the porogen of this process was the DMAc solvent. Increases in the pre-drying time reduced the amount of solvent in the film. The reduction of solvent decreased the pore size and thickness. The variations in the drying time controlled the size of pores in the film.

The electroplating was performed on the surface of the porous PI film. Then, another side of the thin copper film was processed to an electrical circuit. Figure 6 shows an SEM micrograph of the electrical circuit.

The signal circuit was a set of two lines as shown in Figures 6 (a) and 6 (c). The circuit was clearly exposed and adhered well to the porous PI film. As shown in Figure 6 (b), pores were observed throughout the surface of the film. Figure 6 (d) shows the cross-section of the circuit. All pores of the uppermost region of the film were covered with an approximately 50-nm-thick skin layer. The pores were observed through the skin layer of the film because of the high energy of the electron beam during FE-SEM.

In Figure 6 (d), the cross-section of the circuit was warped downward by 2.3 μm. The distance

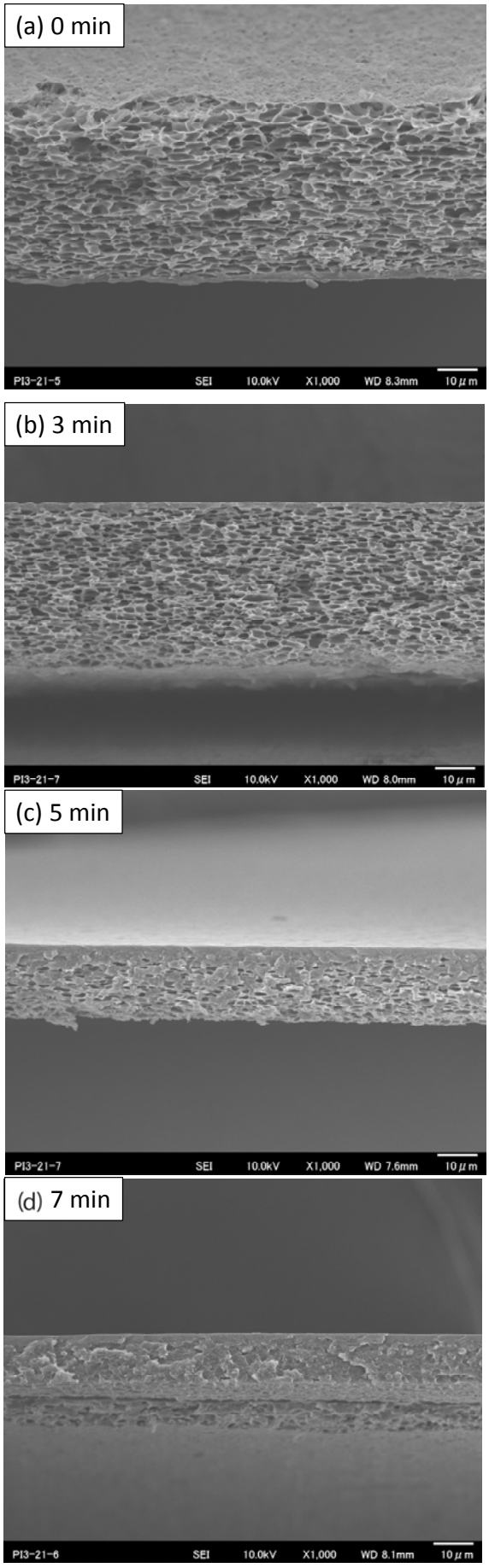

Fig. 5. Effect of pre-drying time on the porous structure.

Table 1. Effect of pre-drying time on the film thickness and porous structure.

Pre-drying time [min]	Thickness [μm]	Pore diameter [μm]
0	44	2.5 ± 0.5
3	41	2.1 ± 0.2
5	18	1.7 ± 0.2
7	12	0.8 ± 0.1

between the bottom of the circuit and the line connecting the edges of circuit was 2.3 μm. The porous polyimide film was prepared by heat-treating the porous polyimide precursor. The film shrunk due to the evaporation of the solvent and imidization of the precursor. The residual stress was stored between the porous polyimide and copper foil. Then, a portion of the copper foil was etched, and the residual stress was released. The foil was warped by the stress that originated from the shrinkage of the porous polyimide film. An electrical circuit of porous polyimide film was successfully prepared.

The signal attenuation of high-frequency electric signals on a porous polyimide substrate was measured and compared with a non-porous polyimide substrate. Figure 7 shows the signal attenuation normalized for 20 mm of electrical circuit. The signal attenuation of both porous and non-porous polyimide decreased with an increasing signal frequency, indicating that the signals were attenuated with an increase in the signal frequency. At 20 GHz, the attenuations of the porous and non-porous polyimide substrates were -0.7 and -1.0 dB/20 min, respectively. The attenuation of porous polyimide was 0.3 dB/20 mm smaller than that of the non-porous polyimide at 20 GHz. Because the porous polyimide contained air, its apparent relative dielectric constant was lower than that of non-porous polyimide.

4. Conclusions

In this study, the production process of large-area porous PI low-k films was developed. It consisted of a fixed window, window holder, high-intensity UV lamp, movable plate and hydraulic press. The maximum working pressure of CO_2 was 6.5 MPa. The maximum temperature was 100 °C. The maximum size of the films produced was ϕ165 mm (6.5 inch), or 150 × 70 mm^2. The process produced porous PI films with 1-10 μm pore sizes, a high porosity and a 40 μm thickness. The porous film is expected to be used

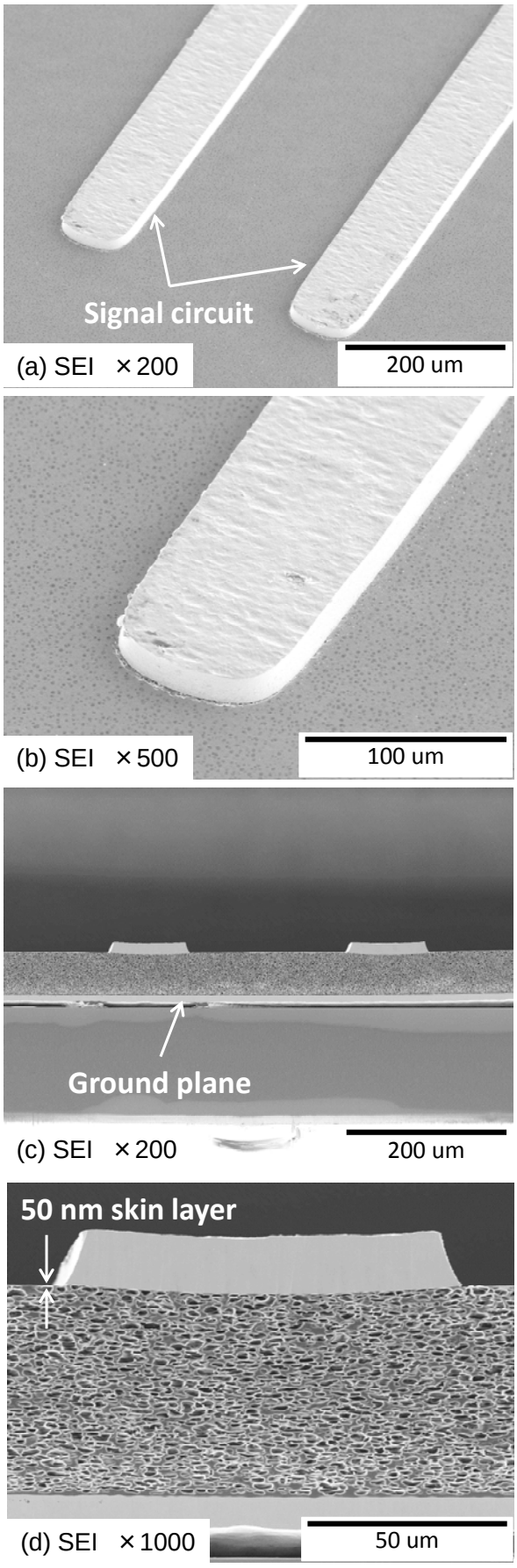

Fig. 6. SEM micrographs of electrical circuits on porous polyimide films prepared using our developed process.

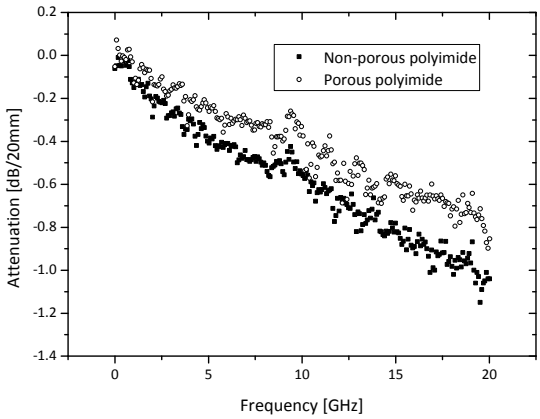

Fig. 7. Signal attenuation of non-porous polyimide and porous polyimide substrates.

for flexible print circuits for high-speed data transmission. Preliminary results of building up a printed circuit on a porous substrate and measurements of signal attenuation at 20 GHz demonstrated that the low-k porous PI substrate reduced the signal attenuation compared with a non-porous substrate of the same cross-sectional area of line. However, the design of electrical circuits for use in the radio frequency range is not as straightforward. It is important to match the characteristic impedance of signal circuits to transmit the signals properly. If the relative dielectric constant of the substrate is reduced, the cross-sectional area of the signal circuit must be decreased to match the characteristic impedance. This increases the loss of resistivity while decreasing the dielectric loss. The total attenuation of the signal is the sum of resistivity and dielectric losses. It is important to reduce not only the dielectric constant but also the loss tangent (tan δ), which is independent of the resistivity loss.

Acknowledgement

The authors are grateful to Mr. Mikami and Mr. Imoto (Imoto Machinery) for their continuous support to develop the apparatus. MULTI, Inc. (Japan) facilitated the development of the electrical circuit. This study was supported by the New Energy and Industrial Technology Development Organization, Japan (NEDO, 09A16003d).

References

1. W. Volksen, R. D. Miller, G. Dubois, *Chem. Rev.*, **110** (2009) 56.
2. M. H. Weng, H. W. Wu, Y. K. Su, R. Y. Yang, C. Y. Hung, *Microwave Opt. Technol. Lett.*, **48** (2006)

1675.
3. H. W. Wu, Y. K. Su, R. Y. Yang, M. H. Weng, Y. D. Lin, *Microelectron. J.*, **38** (2007) 304.
4. Y. Ren, D. C. C. Lam, *J. Electron. Mater*., **37** (2008) 955.
5. X.-Y. Zhao, H.-J. Liu, *Polym. Int.*, **59** (2010) 597.
6. S. Ma, Y. Wang, Z. Min, L. Zhong, *Adv. Polym. Tech.*, **32** (2013) 21358.
7. J. L. Hedrick, K. R. Carter, J. W. Labadie, R. D. Miller, W. Volksen, C. J. Hawker, D. Y. Yoon, T. P. Russell, J. E. McGrath, R. M. Briber, *Progress in Polyimide Chemistry II* (Ed: H. R. Kricheldorf), Springer, Berlin Heidelberg (1999), p. 1.
8. B. Krause, K. Diekmann, N. F. A. van der Vegt, M. Wessling, *Macromolecules*, **35** (2002) 1738.
9. B. Krause, G. H. Koops, N. F. A. van der Vegt, M. Wessling, M. Wubbenhorst, J. van Turnhout, *Adv. Mater.*, **14** (2002) 1041.
10. A. Mochizuki, T. Fukuoka, M. Kanada, N. Kinjou, T. Yamamoto, *J. Photopolym. Sci. Technol*., **15** (2002) 159.
11. F. Lv, L. Liu, Y. Zhang, P. Li, *J. Appl. Polym. Sci.*, **132** (2015) 41480.
12. Y. J. Lee, J. M. Huang, S. W. Kuo, F. C. Chang, *Polymer*, **46** (2005) 10056.
13. Y. J. Lee, J. M. Huang, S. W. Kuo, J. S. Lu, F. C. Chang, *Polymer*, **46** (2005) 173.
14. M. A. Wahab, K. Y. Mya, C. B. He, *J. Polym. Sci., Part A: Polym. Chem.*, **46** (2008) 5887.
15. S. Devaraju, M. R. Vengatesan, M. Selvi, A. A. Kumar, M. Alagar, *High Perform. Polym.*, **24** (2012) 85.
16. J. J. Lin, X. D. Wang, *Polymer*, **48** (2007) 318.
17. Z. M. Dang, L. J. Ma, J. W. Zha, S. H. Yao, D. Xie, Q. Chen, X. Duan, *J. Appl. Phys.*, **105** (2009) 044104.
18. G. F. Zhao, T. Ishizaka, H. Kasai, M. Hasegawa, T. Furukawa, H. Nakanishi, H. Oikawa, *Chem. Mater.*, **21** (2009) 419.
19. A. Bittner, H. Seidel, U. Schmid, *Microelectron. Eng.*, **88** (2011) 2977.
20. J. Im, S. Y. Hong, Y. Cheon, J. Lee, J. S. Lee, H. S. Kim, M. Cheong, H. Park, *Energy Environ. Sci.* **4** (2011) 4284.
21. Y. X. Jin, J. Tang, J. Hu, X. Han, Y. Z. Shang, H. L. Liu, *Colloids Surf. A*, **392** (2011) 178.
22. S. Chisca, I. Sava, M. Bruma, *Polym. Int*., **62** (2013) 1634.
23. K. Taki, S. Okumura, *Macromolecules*, **43** (2010) 9899.
24. R. Okaji, K. Taki, S. Nagamine, M. Ohshima, *J. Appl. Polym. Sci.*, **125** (2012) 2874.
25. K. Taki, K. Hosokawa, S. Takagi, H. Mabuchi, M. Ohshima, *Macromolecules*, **46** (2013) 2275.